Integrated Motion Planning, Control, and Estimation for Range-Based Marine Vehicle Positioning and Target Localization

D. Moreno-Salinas * **N. Crasta** ** **M. Ribeiro** ** **B. Bayat** ***
A. M. Pascoal ** **J. Aranda** *

* *Department of Computer Science and Automatic Control, National Distance Education University, Madrid, Spain.* {*dmoreno,jaranda*}*@dia.uned.es*
** *Laboratory of Robotics and Systems in Engineering and Science(LARSyS), ISR/IST, University of Lisbon, Lisbon, Portugal* {*ncrasta,miguel.silva.ribeiro,antonio*}*@isr.tecnico.ulisboa.pt*
*** *BioRobotics Laboratory, Ecole Polytechnique Fédérale de Lausanne (EPFL), Switzerland. behzad.bayat@epfl.ch.*

Abstract: The paper addresses the problems of range-based marine vehicle positioning and target localization. *Vehicle positioning* aims to estimate the positions of one or more vehicles from a sequence of range measurements to fixed or moving acoustic beacons with known locations. In this context, the vehicles must execute sufficiently exciting maneuvers so as to maximize the range-based information available for multiple vehicle positioning. Using an estimation theoretical setting, the vehicle trajectories are computed by maximizing the determinant of a suitably defined Fisher information matrix (FIM), subject to inter-vehicle collision avoidance and vehicle maneuvering constraints. A numerical solution is proposed for the general case. Analytical solutions are obtained in the case of one vehicle and one beacon, when the latter undergoes trajectories that are straight lines, pieces of arcs, or a combination thereof. The theoretical analysis is complemented with practical experiments that focus on the dual problem of underwater *target localization*. The objective is to estimate the position of a moving underwater target by using range measurements between the target and a vehicle, called a tracker, undergoing a trajectory that can be measured on-line. The experimental set-up includes a surface and an autonomous underwater vehicle of the MEDUSA[1]-class playing the roles of tracker and target, respectively. In the methodology adopted for system implementation the tracker runs three key algorithms simultaneously, over a sliding time window: i) tracker motion planning, ii) tracker motion control, and iii) target motion estimation based on range data acquired on-line.

Keywords: Underwater range-based navigation, Single-beacon localization, Trajectory optimization, Fisher information matrix.

1. INTRODUCTION

Autonomous underwater vehicles (AUVs) have steadily become an important tool to carry out a large number of scientific and commercial missions at sea. Among the systems required for reliable AUV operation, vehicle positioning plays a critical role. Recently, with the advent of miniaturized sensors and the availability of small embedded processors, there has been tremendous interest in the development of positioning systems that are cost-effective and easy to install and operate. The latter include range-based positioning systems, which have emerged as viable alternatives to conventional acoustic methods such as long baseline (LBL) and ultra short baseline (USBL) systems in a large number of operational scenarios.

In its simplest form, a range-based positioning system aims to estimate the position of an underwater vehicle from a sequence of range measurements to an acoustic beacon with a known location. The reader is referred to (Webster et al., 2013), (Crasta, 2015) and (Bayat, 2016) for fast paced expositions of challenging theoretical and practical issues that arise in this context. The work in (Webster et al., 2013) deals with the design and experimental testing of a decentralized filter for single-beacon cooperative acoustic navigation. In (Crasta, 2015), the authors study the observability properties of the kinematic model of an autonomous underwater vehicle moving in 3D, under the influence of ocean currents, using range and depth measurements. The analysis is done under the assumption that the AUV undergoes trimming trajectories. The work in (Bayat, 2016) discusses important observability results and introduces a multi-model adaptive observer methodology to solve the problem of range-based autonomous underwater vehicle localization in the presence of unknown ocean currents. This is done for the more general case where the AUV measures its distance to a set of stationary beacons whose number is not known a-priori.

In the set-up considered in this paper, the types of trajectories that a vehicle executes impact directly on the level of accuracy with which its position can be estimated. In summary, the vehicle must execute sufficiently exciting

⋆ The work of N. Crasta and M. Ribeiro was supported by the European Commission through the CADDY Project (FP7-ICT-2013) under Grant 611373.
⋆⋆The work of D. Moreno-Salinas and J. Aranda was supported by "Ministerio de Economia y Competitividad" under project DPI2013-46665-C2-2-R.
⋆ ⋆ ⋆The work of B. Bayat was supported by Envirobot, a project of the Swiss NanoTera program.
[1] MEDUSA is an AUV developed and operated by the Institute for Systems and Robotics of IST.

maneuvers so as to maximize the range-based information available for vehicle positioning. In this respect, the problem has interesting connections with the by now classical dual problem of optimal, fixed sensor placement for target localization. See for example (Moreno-Salinas et al., 2016), where an analytical result on optimal sensor placement for target localization is given, together with the geometrical interpretation of the solutions obtained. By adopting an estimation theoretical setting, appropriate vehicle trajectories can be computed by maximizing the determinant of a suitably defined Fisher information matrix (FIM), searching over a number of appropriately chosen, motion-related variables that parameterize the trajectories. The reader is referred to (Margarida et al., 2015) and the references therein for an introduction to this technique that uses the FIM as a performance index. The empirical observability Grammian has also been used in the literature as an alternative performance index, but as shown in (Powel et al., 2015) the two are related.

It is against this background of ideas that in the present paper we address the general problem of multiple vehicle range-based positioning, where the objective is to estimate the position of one or more vehicles from a sequence of range measurements to single or multiple acoustic beacons with fixed or time-varying known positions. Optimal vehicle trajectories are computed by maximizing the determinant of a suitably defined Fisher information matrix (FIM), subject to inter-vehicle collision avoidance and vehicle maneuvering constraints. A numerical solution is proposed for the general case. Analytical solutions are obtained in the case of one vehicle and one beacon, when the latter undergoes trajectories that are straight lines, pieces of arcs, or a combination thereof. The theoretical analysis is complemented with practical experiments that focus on the dual problem of underwater target localization. The objective is to estimate the position of a moving underwater target by using range measurements between the target and a vehicle, called a tracker, undergoing a trajectory that can be measured on-line. The experimental set-up includes a surface and an autonomous underwater vehicle of the MEDUSA-class that play the roles of tracker and target, respectively. In the methodology adopted for system implementation the tracker runs three key algorithms simultaneously, over a sliding time window: i) tracker motion planning, ii) tracker motion control, and iii) target motion estimation based on range data acquired on-line.

The paper is organized as follows. Section 2 introduces some basic notation. The problem formulation is given in Section 3. Section 4 deals with the computation of the FIM for the problem at hand, while Section 5 describes the analytical construction of optimal vehicle trajectories for one vehicle and one beacon case. Section 6 describes the experimental set-up adopted for target localization and validates the efficacy of the method proposed. Finally, Section 7 contains the main conclusions.

2. PRELIMINARIES

Given $n \in \mathbb{N}$, we define $\mathbb{I}_n := \{1, \dots, n\}$. Given $p \geq 1$, $q \geq 1$, and $m \geq 2$, throughout the paper we use $i \in \mathbb{I}_p$, $\alpha \in \mathbb{I}_q$, and $k \in \{0\} \cup \mathbb{I}_{m-1}$ to denote the i^{th} vehicle, the α^{th} beacon, and the k^{th} sample, respectively. We denote the Euclidean norm in $\mathbb{R}^n$ by $\|\cdot\|$ and the unit sphere in $\mathbb{R}^n$ by S^n, that is, $\mathrm{S}^n := \{\mathbf{x} \in \mathbb{R}^n \colon \|\mathbf{x}\| = 1\}$. We define two orthogonal unit vectors $\mathbf{g} \colon [0, 2\pi) \to \mathrm{S}^1$ and $\mathbf{g}^\perp \colon [0, 2\pi) \to \mathrm{S}^1$ by $\mathbf{g}(\theta) = [\cos\theta \ \sin\theta]^{\mathrm{T}}$ and $\mathbf{g}^\perp(\theta) = [-\sin\theta \ \cos\theta]^{\mathrm{T}}$, $\theta \in [0, 2\pi)$, respectively. Further, we denote the identity matrix of size n by I_n and by $\mathbf{0}_{m\times n}$ we mean the zero matrix of size $m \times n$. Given $\mathbf{w} \in \mathbb{R}^n$, $\mathrm{diag}(\mathbf{w}) \in \mathbb{R}^{n\times n}$ denotes the diagonal matrix whose diagonal elements are the components of the vector $\mathbf{w}$. In a similar fashion, given $n, s \in \mathbb{N}$ and $A_j \in \mathbb{R}^{n\times n}$, $j \in \mathbb{I}_s$, we can define $\mathrm{diag}(A_1, \dots, A_s)$, and we denote the direct sum of $A_1, \dots, A_s$ by $\bigoplus_{j\in\mathbb{I}_s} A_j := \mathrm{diag}(A_1, \dots, A_s)$. Finally, given a smooth function $f \colon \mathbb{R}^n \to \mathbb{R}$, the gradient of f is denoted by ∇f. Unless indicated otherwise, gradient vector in the paper will be a column vector.

3. PROBLEM FORMULATION

Consider $p \in \mathbb{N}$ vehicles and $q \in \mathbb{N}$ beacons. In the absence of ocean currents, the kinematics model (Margarida et al., 2015) for the i^{th} vehicle, $i \in \mathbb{I}_p$, (see Fig. 1), is given by

$$\dot{\mathbf{p}}^{[i]} = \begin{bmatrix} \cos(\chi^{[i]}) & -\sin(\chi^{[i]}) \\ \sin(\chi^{[i]}) & \cos(\chi^{[i]}) \end{bmatrix} \begin{bmatrix} v^{[i]} \\ 0 \end{bmatrix}, \tag{1}$$

$$\dot{\chi}^{[i]} = r^{[i]}, \tag{2}$$

where $t \in [0, t_f]$, $\mathbf{p}^{[i]} \in \mathbb{R}^2$ is the instantaneous inertial position vector of the i^{th} vehicle, $\chi^{[i]} \colon [0, t_f] \to [0, 2\pi)$ is the (relative) course angle of the i^{th} vehicle that gives the orientation of the flow-frame with respect to an inertial frame, $v^{[i]} \colon [0, t_f] \to [0, \infty)$ is the speed of the i^{th} vehicle with respect to the water, i.e. $v^{[i]} \equiv \|\mathbf{v}^{[i]}\|$, and $r^{[i]} \colon [0, t_f] \to \mathbb{R}$ its (relative) course-rate. In what follows, with an obvious abuse of the notation, we will refer to relative course angle and relative course rate simply as course angle and course rate, respectively. In state-space formulation $\mathbf{x}^{[i]} := (\mathbf{p}^{[i]}, \chi^{[i]}) \in \mathcal{M} := \mathbb{R}^2 \times [0, 2\pi)$ is the state vector and $\mathbf{u}^{[i]} := (v^{[i]}, r^{[i]}) \in \mathcal{U} := [0, \infty) \times \mathbb{R}$ is the input.

In order to avoid collisions, the vehicles must satisfy

$$\|\mathbf{p}^{[i]}(t) - \mathbf{p}^{[j]}(t)\| \geq R, \ i, j \in \mathbb{I}_p, \ i < j,$$
$$\|\mathbf{p}^{[i]}(t) - \mathbf{b}^{[\alpha]}(t)\| \geq R, \ i \in \mathbb{I}_p, \ \alpha \in \mathbb{I}_q,$$

for all $t \in [0, t_f]$, where $R > 0$ is a safety radius. Each vehicle is equipped with sensors that measure distances to a set of fixed/moving beacons $\mathcal{B} := \{\mathbf{b}^{[1]}, \dots \mathbf{b}^{[q]}\} \subset \mathbb{R}^2$, the inertial positions of which are described by known functions of time, see Fig. 1. For each $i \in \mathbb{I}_p$ and $\alpha \in \mathbb{I}_q$, let $\mathbf{d}^{[\alpha i]}$ denote the relative position vector of the i^{th} AUV

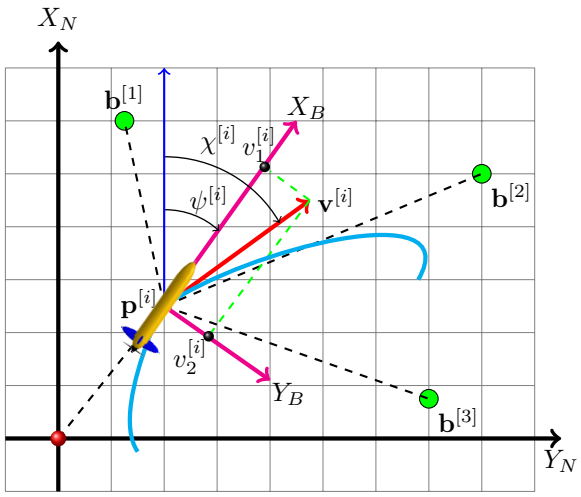

Fig. 1. Illustration of an AUV with three beacons, where $\psi^{[i]}$ is the heading angle and $\chi^{[i]}$ is the course angle.

with respect to the α^{th} beacon $\mathbf{b}^{[\alpha]}$, that is, $\mathbf{d}^{[\alpha i]} := \mathbf{p}^{[i]} - \mathbf{b}^{[\alpha]}$ and let $d_{\alpha i} := \|\mathbf{d}^{[\alpha i]}\|$ denote the corresponding distance. The instantaneous measurements of distances collected at time $t \in [0, t_f]$, denoted $Y(t)$, are corrupted by additive white Gaussian noise as follows:

$$Y(t) = D(t) + \eta(t),$$

where $D \in \mathbb{R}^{q\times p}$ (the matrix of true instantaneous distances) and $\eta \in \mathbb{R}^{q\times p}$ are given by

$$D := \begin{bmatrix} d_{11} & \cdots & d_{1p} \\ \vdots & \ddots & \vdots \\ d_{q1} & \cdots & d_{qp} \end{bmatrix}, \quad \eta := \begin{bmatrix} \eta_{11} & \cdots & \eta_{1p} \\ \vdots & \ddots & \vdots \\ \eta_{q1} & \cdots & \eta_{qp} \end{bmatrix},$$

and $\eta_{\alpha i} \sim \mathcal{N}(0, \sigma_{\alpha i}^2)$, $\alpha \in \mathbb{I}_q$, $i \in \mathbb{I}_p$.

The solution to (1)-(2) at time $t \in [0, t_f]$ for the initial condition $\mathbf{x}_0^{[i]} = (\mathbf{p}_0^{[i]}, \chi_0^{[i]}) \in \mathcal{M}$ and the input $\mathbf{u}^{[i]} = (v^{[i]}, r^{[i]})$ can be written as

$$\mathbf{x}^{[i]}(t) = \mathbf{x}_0^{[i]} + \left(\int_0^t v^{[i]}(\tau)\mathbf{g}(\chi^{[i]}(\tau))\mathrm{d}\tau, \int_0^t r^{[i]}(\tau)\mathrm{d}\tau \right).$$

Let $t_f > 0$ and $m \in \mathbb{N}$, $m \geq 2$. Consider a strictly monotonically increasing time sequence $\{t_k\}_{k=0}^{m-1} \subseteq [0, t_f]$ of length m with $t_0 := 0$ and $t_{m-1} := t_f$. To simplify the notation, we let $\mathbf{p}_k^{[i]} := \mathbf{p}^{[i]}(t_k)$, $\chi_k^{[i]} := \chi^{[i]}(t_k)$, $\mathbf{g}_k^{[i]} := \mathbf{g}(\chi^{[i]}(t_k))$, $Y_k := Y(t_k)$, $D_k := D(t_k)$, and $\eta_k := \eta(t_k)$. Then, for each $k \in \{0\} \cup \mathbb{I}_{m-2}$, (1)-(2) can be written as

$$\mathbf{x}_{k+1}^{[i]} = \mathbf{x}_k^{[i]} + \left(\int_{t_k}^{t_{k+1}} v^{[i]}(\tau)\mathbf{g}(\chi^{[i]}(\tau))\mathrm{d}\tau, \int_{t_k}^{t_{k+1}} r^{[i]}(\tau)\mathrm{d}\tau \right). \quad (3)$$

We assume that the vehicle's speed and course-rate are piece-wise constant functions, and speed as well as course-rate are bounded (above and below), that is, for all $k \in \{0\} \cup \mathbb{I}_{m-2}$ and $t \in [t_k, t_{k+1})$,

$$(v^{[i]}(t), r^{[i]}(t)) \equiv (\bar{v}_k^{[i]}, \bar{r}_k^{[i]}) \in [0, \bar{v}_{\text{ub}}] \times [-\bar{r}_{\text{ub}}, \bar{r}_{\text{ub}}].$$

Define $\bar{\lambda}_k^{[i]} := \bar{v}_k^{[i]}/\bar{r}_k^{[i]}$, whenever $\bar{r}_k^{[i]} \neq 0$. With these assumptions, for each $k \in \{0\} \cup \mathbb{I}_{m-2}$, the second component of (3) can be reduced to

$$\chi^{[i]}(t) = \chi_k^{[i]} + (t - t_k)\bar{r}_k^{[i]},\ t \in [t_k, t_{k+1})$$

and using the last equation in the first component of (3) we get

$$\mathbf{p}^{[i]}(t) = \mathbf{p}_k^{[i]} + \bar{\lambda}_k^{[i]} \left[\left(\mathbf{g}_k^{[i]}\right)^{\perp} - \left(\mathbf{g}(\chi^{[i]}(t))\right)^{\perp} \right].$$

In particular, for each $k \in \{0\} \cup \mathbb{I}_{m-2}$,

$$\mathbf{p}_{k+1}^{[i]} = \mathbf{p}_k^{[i]} + \bar{\lambda}_k^{[i]} \left[\left(\mathbf{g}_k^{[i]}\right)^{\perp} - \left(\mathbf{g}_{k+1}^{[i]}\right)^{\perp} \right],$$

or equivalently, for $k \in \{0\} \cup \mathbb{I}_{m-2}$,

$$\mathbf{p}_{k+1}^{[i]} = \mathbf{p}_0^{[i]} + \textstyle\sum_{j=0}^{k} \bar{\lambda}_j^{[i]} \left[\left(\mathbf{g}_k^{[i]}\right)^{\perp} - \left(\mathbf{g}_{k+1}^{[i]}\right)^{\perp} \right]. \quad (4)$$

With this set-up, we now formulate the following question: *"Given the time-history of the beacon positions defined over a fixed time interval, what is the sequence of actions for each of the AUVs (in terms of vehicle speed and course rate) that will collectively maximize the information available to compute their initial positions"?*

In what follows we answer this question by adopting the classical set-up of estimation theory that hinges on the computation of a suitably defined FIM matrix.

4. FISHER INFORMATION MATRIX

In this section we derive the FIM for the model described before, consisting of the vehicle kinematics and measurement equations. The objective is to estimate the initial positions of the AUVs. As is well known, the inverse of the FIM is instrumental in computing a lower bound on the covariance of the estimates of a deterministic parameter that can be achieved with any unbiased estimator. This result yields the celebrated Cramér-Rao Lower Bound (Van Trees, 1968), which we seek to reduce by maximizing the determinant of the FIM.

For a given number of samples m, with input sequence $\mathbf{U} := (u_0, \ldots, u_{m-1})$, and an unknown parameter $\boldsymbol{\theta} \in \mathbb{R}^n$, we denote the corresponding FIM by $FIM_{\mathbf{U}}(\boldsymbol{\theta}) \in \mathbb{R}^{n\times n}$. The FIM with respect to the unknown parameter of interest $\boldsymbol{\theta}$ is given by

$$FIM_{\mathbf{U}}(\boldsymbol{\theta}) := \mathbb{E}\left\{ \left[\nabla_{\boldsymbol{\theta}} \left(\log \mathcal{L}_{\boldsymbol{\theta}}(\mathbf{y})\right)\right] \left[\nabla_{\boldsymbol{\theta}} \left(\log \mathcal{L}_{\boldsymbol{\theta}}(\mathbf{y})\right)\right]^{\mathrm{T}} \right\},$$

where $\mathbf{y} \in \mathbb{R}^m$ is the measurement vector, $\mathcal{L}_{\boldsymbol{\theta}}(\mathbf{y})$ is the likelihood function of the measurement with respect to the parameter $\boldsymbol{\theta}$, and $\mathbb{E}$ is the expectation operator. To maximize the FIM, we define a scalar function

$$J(\mathbf{U}) := \ln\det(FIM_{\mathbf{U}}(\boldsymbol{\theta})),$$

which is equivalent to minimizing $\ln\det((FIM_{\mathbf{U}}(\boldsymbol{\theta}))^{-1})$, that is, $-J(\mathbf{U})$. With this background, we next derive the FIM for the problem under consideration.

For the sake of simplicity, in the sequel we use the following compact notation:

$$\widehat{\mathcal{P}}_{\alpha}^{[i]} := \left[(d_{\alpha i,0})^{-1}\mathbf{d}_0^{[\alpha i]} \ \cdots \ (d_{\alpha i,m-1})^{-1}\mathbf{d}_{m-1}^{[\alpha i]} \right] \in \mathbb{R}^{2\times m},$$
$$\boldsymbol{v}^{[i]} := (\bar{v}_0^{[i]}, \ldots, \bar{v}_{m-2}^{[i]}) \in [0, \bar{v}_{\text{ub}}]^{m-1},$$
$$\boldsymbol{r}^{[i]} := (\bar{r}_0^{[i]}, \ldots, \bar{r}_{m-2}^{[i]}) \in [-\bar{r}_{\text{ub}}, \bar{r}_{\text{ub}}]^{m-1},$$
$$\mathbf{U}_i := \left(\boldsymbol{v}^{[i]}, \boldsymbol{r}^{[i]}\right).$$

4.1 FIM for a single vehicle

First we derive the FIM for a single vehicle with q beacons. Consider the i^{th} AUV motion described by (4) with the output equation given by

$$\mathbf{y}_k^{[i]} = \mathbf{d}_k^{[i]} + \eta_k^{[i]},$$

where $\mathbf{d}_k^{[i]}$ and $\eta_k^{[i]}$ are the i^{th} columns of D_k and η_k, respectively. In this particular case, we have $\boldsymbol{\theta}_i = \mathbf{p}_0^{[i]}$ and we let $FIM_{\mathbf{U}_i}^{[i]}(\boldsymbol{\theta}_i) \in \mathbb{R}^{2\times 2}$ denote the FIM for this set-up. Following a standard procedure, we have

$$FIM_{\mathbf{U}_i}^{[i]}(\boldsymbol{\theta}_i) = \sum_{\alpha\in\mathbb{I}_q} \sum_{k\in\{0\}\cup\mathbb{I}_{m-1}} \sigma_{\alpha i}^{-2} \left(\nabla_{\boldsymbol{\theta}_i} d_{\alpha i,k}\right) \left(\nabla_{\boldsymbol{\theta}_i} d_{\alpha i,k}\right)^{\mathrm{T}}, \quad (5)$$

where

$$\nabla_{\boldsymbol{\theta}_i} d_{i\alpha,k} = (d_{i\alpha,k})^{-1}\, \mathbf{d}_k^{[i\alpha]} \in \mathbb{R}^2. \quad (6)$$

Substituting (6) into (5), and simplifying further yields

$$FIM_{\mathbf{U}_i}^{[i]}(\boldsymbol{\theta}_i) = \sum_{\alpha\in\mathbb{I}_q} \sigma_{\alpha i}^{-2}\ \widehat{\mathcal{P}}_{\alpha}^{[i]} (\widehat{\mathcal{P}}_{\alpha}^{[i]})^{\mathrm{T}}.$$

Notice that $\mathrm{trace}(\widehat{\mathcal{P}}_{\alpha}^{[i]} (\widehat{\mathcal{P}}_{\alpha}^{[i]})^{\mathrm{T}}) = m$. Consequently,

$$\mathrm{trace}(FIM_{\mathbf{U}_i}^{[i]}(\boldsymbol{\theta}_i)) = m \sum_{\alpha\in\mathbb{I}_q} \sigma_{\alpha i}^{-2}.$$

4.2 FIM for multiple vehicles

We next derive the FIM for more than one vehicle. In this particular case, we have $\mathbf{U} := (\mathbf{U}_1, \ldots, \mathbf{U}_p)$, $\boldsymbol{\theta} := (\boldsymbol{\theta}_1, \ldots, \boldsymbol{\theta}_p)$ and we let $FIM_{\mathbf{U}}(\boldsymbol{\theta}) \in \mathbb{R}^{2p\times 2p}$ denote the FIM for this set-up. The FIM for the complete system is given by

$$FIM_{\mathbf{U}}(\boldsymbol{\theta}) = \sum_{i\in\mathbb{I}_p}\sum_{\alpha\in\mathbb{I}_q}\sum_{k\in\{0\}\cup\mathbb{I}_{m-2}} \sigma_{\alpha i}^{-2}\left(\nabla_{\boldsymbol{\theta}} d_{\alpha i,k}\right)\left(\nabla_{\boldsymbol{\theta}} d_{\alpha i,k}\right)^{\mathrm{T}},$$

where

$$\nabla_{\boldsymbol{\theta}} d_{\alpha i,k} = \frac{1}{d_{\alpha i,k}}\begin{bmatrix}\mathbf{0}_{2(i-1)\times 1}\\ \nabla_{\boldsymbol{\theta}_i} d_{\alpha i,k}\\ \mathbf{0}_{2(p-i)\times 1}\end{bmatrix} \in \mathbb{R}^{2p}.$$

Simplifying further yields

$$FIM_{\mathbf{U}}(\boldsymbol{\theta}) = \bigoplus_{i\in\mathbb{I}_p} FIM_{\mathbf{U}_i}^{[i]}(\boldsymbol{\theta}_i).$$

Note that the overall FIM depends on $\boldsymbol{v}^{[1]}, \ldots, \boldsymbol{v}^{[p]}$ and $\boldsymbol{r}^{[1]}, \ldots, \boldsymbol{r}^{[p]}$. We now compute the maximum value of the FIM determinant.

4.3 Optimal FIM determinant

In this section we examine the optimum value of the cost functional described by

$$J(\mathbf{U}) = \ln\det(FIM_{\mathbf{U}}(\boldsymbol{\theta})) = \textstyle\sum_{i\in\mathbb{I}_p} \ln\det(FIM_{\mathbf{U}_i}^{[i]}(\boldsymbol{\theta}_i)).$$

In the above equation, the second equality follows by noting that

$$\det\left(\bigoplus_{i\in\mathbb{I}_p} FIM_{\mathbf{U}_i}^{[i]}(\boldsymbol{\theta}_i)\right) = \prod_{i\in\mathbb{I}_p}\det(FIM_{\mathbf{U}_i}^{[i]}(\boldsymbol{\theta}_i)).$$

Thus, it suffices to maximize the FIM associated with each of the vehicles in order to maximize the overall FIM. The following result is obtained.

Proposition 1. Consider $i \in \mathbb{I}_p$ and assume that $\sigma_{\alpha i} := \sigma$ for all $\alpha \in \mathbb{I}_q$. Let

$$\sum_{\alpha\in\mathbb{I}_q} \widehat{\mathcal{P}}_{\alpha}^{[i]}(\widehat{\mathcal{P}}_{\alpha}^{[i]})^{\mathrm{T}} = \left(\frac{qm}{2}\right) I_2.$$

Then, $\det(FIM_{\mathbf{U}_i}^{[i]}(\boldsymbol{\theta}_i))$ is maximum and given by $\left(2^{-1}\sigma^{-2}qm\right)^2$; consequently, the optimal value of $\det(FIM_{\mathbf{U}}(\boldsymbol{\theta}))$ is given by $\left(2^{-1}\sigma^{-2}qm\right)^{2p}$.

Proof. The proof is based on the results in (Moreno-Salinas et al., 2013).

So far we have derived the optimal value for the cost functional adopted, but we have provided no insight into the optimal trajectories of the vehicles. In general, it is not possible to characterize these trajectories analytically (this is possible, however for the case of a single vehicle and a single beacon). For this reason, we resort to numerical optimization methods to compute the optimal vehicle trajectories that maximize the determinant of FIM, subject to collision and vehicle maneuvering constraints. In the following subsection all optimizations are performed using the *simulated annealing technique.* *

* Global Optimization Toolbox: Simulated Annealing, `http://es.mathworks.com/help/gads/index.html`, The MathWorks, Inc., 1994-2016.

4.4 Numerical example

We consider $p = 3$, $q = 1$, and $\mathbf{b}^{[1]}(t) \equiv \mathbf{0}$. Recall from Proposition 1 that the optimal FIM for each vehicle is given by $400I_2$ and overall optimal FIM determinant is given by 4.0960×10^{15}. The simulation parameters are $\mathbf{p}_0^{[1]} = [-15 \quad 0]^{\mathrm{T}}$[m], $\mathbf{p}_0^{[2]} = [15 \quad 0]^{\mathrm{T}}$[m], $\mathbf{p}_0^{[3]} = [10 \quad 15]^{\mathrm{T}}$[m], $v^{[1]} = v^{[2]} = v^{[3]} = 2$ [m/s], $R = 5$ [m], $T = 6$ [s], $\sigma = 0.1$ [m], and $m = 8$. Fig. 2 shows the optimal trajectories for each of the vehicles, while Fig. 3 shows the corresponding optimal course-rates. The FIM obtained from the simulations is $FIM_{\mathbf{U}_i}^{[i]}(\boldsymbol{\theta}_i) = 400I_2$, $i \in \mathbb{I}_3$.

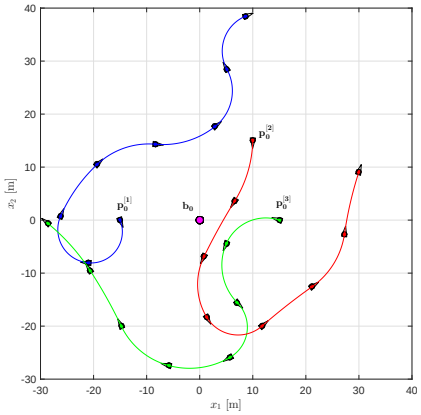

Fig. 2. Optimal trajectories of three vehicles for a fixed beacon at the origin.

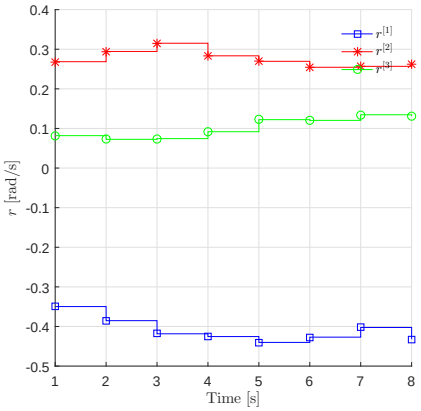

Fig. 3. Optimal course rates for the three vehicles.

In the following section, we focus on the single-beacon positioning problem.

5. OPTIMAL TRAJECTORIES: SINGLE-BEACON CASE

In this section we consider $p = q = 1$, and for this particular case we provide a constructive analytical solution. In the sequel all the optimal variables are denoted with the superscript " $*$ ".

i) Let $\mathbf{p}_0 \in \mathbb{R}^2$ and $\mathbf{b}_0 \in \mathbb{R}^2$ denote the initial position of the vehicle and beacon, respectively.
ii) Let $m \geq 3$ be the number of samples; we assume uniform sampling, that is, $t_k = kT$, $k \in \{0\} \cup \mathbb{I}_{m-1}$. Define $\beta_k := \beta_0 - m^{-1}\lambda k\pi$, ** $k \in \mathbb{I}_{m-1}$, $\lambda \in \{1, 2\}$, where β_0 is the angle between the vector $\mathbf{p}_0 - \mathbf{b}_0$ and

** In rest of the paper we assume $\lambda = 1$.

the horizontal axis Y_N. Assume piecewise constant vehicle speed and course rate, that is, for $k \in \{0\} \cup \mathbb{I}_{m-2}$,

$$(v(t), r(t)) \equiv (\bar{v}_k, \bar{r}_k), \ t \in [t_k, t_{k+1}).$$

iii) Fix $k \in \mathbb{I}_{m-2}$. Finding the optimal position $\mathbf{p}_k^*$ consists of the following steps:

a) Recall that $\mathbf{d}_k = \mathbf{p}_k - \mathbf{b}_k$ and $d_k = \|\mathbf{d}_k\|$. Let $\mathbf{p}_k = \mathbf{b}_k + d_k \mathbf{g}(\beta_k)$, $k \geq 1$, where $d_k \in \mathbb{R}$ is an unknown constant that needs to be determined and let $\mathbf{p}_0^* = \mathbf{p}_0$.

b) Solve the following equation for d_k:

$$\|\mathbf{p}_k - \mathbf{p}_{k-1}^*\|^2 = (a_k)^2, \ k \geq 1, \tag{7}$$

where $a_k := \bar{v}_{k-1}(t_k - t_{k-1}) = T\bar{v}_{k-1}$. Here for the time being we assume $\bar{v}_{k-1}$ to be the nominal speed of the vehicle (which is within the bounds). Equation (7) is equivalent to

$$d_k^2 + 2d_k(\mathbf{b}_k - \mathbf{p}_{k-1}^*)^{\mathrm{T}}\mathbf{g}(\beta_k) + \|\mathbf{b}_k - \mathbf{p}_{k-1}^*\|^2 - (a_k)^2 = 0,$$

which is quadratic in the unknown variable d_k. To ensure real solutions we need to satisfy $(a_k)^2 - \left(\|\mathbf{b}_k - \mathbf{p}_{k-1}^*\| \sin\theta_k\right)^2 \geq 0$, where $\theta_k \in [0, \pi]$ is the angle between vectors $(\mathbf{b}_k - \mathbf{p}_{k-1}^*)$ and $\mathbf{g}(\beta_k)$. The real roots are given by

$$d_k = -\|\mathbf{b}_k - \mathbf{p}_{k-1}^*\| \cos\theta_k \pm \sqrt{(a_k)^2 - \left(\|\mathbf{b}_k - \mathbf{p}_{k-1}^*\| \sin\theta_k\right)^2}.$$

c) Following Moreno-Salinas et al. (2016), among the two real solutions for d_k, we select the one with the larger magnitude, say d_k^*.

d) The optimal position is given by

$$\mathbf{p}_k^* = \mathbf{b}_k + d_k^* \mathbf{g}(\beta_k).$$

e) This construction leads to the optimal solution because

$$\begin{aligned} FIM_{\mathbf{U}^i}^{[i]}(\boldsymbol{\theta}_i) &= \sigma^{-2} \sum_{k \in \{0\} \cup \mathbb{I}_{m-1}} \left(\frac{\mathbf{d}_k^*}{d_k^*}\right) \left(\frac{\mathbf{d}_k^*}{d_k^*}\right)^{\mathrm{T}}, \\ &= \sigma^{-2} \sum_{k \in \{0\} \cup \mathbb{I}_{m-1}} \mathbf{g}(\beta_k)\mathbf{g}(\beta_k)^{\mathrm{T}} \\ &= \left(m\sigma^{-2}/2\right) I_2, \end{aligned}$$

where the last equality follows from the orthogonality of the sine and cosine functions.

f) Now that the optimal positions are computed, the piecewise constant $\bar{v}_k^*$ and $\bar{r}_k^*$ are determined so that those positions are reached in a smooth manner and at the appropriate instants of time.

In the sequel, we use the above algorithm to show what types of optimal solutions are obtained for straight-line and circular motions of the beacon.

5.1 Straight-line motion

In this case, we consider a beacon moving along the unit vector $\mathbf{w} \in \mathrm{S}^2$ with a constant forward speed of v_b starting from $\mathbf{b}_0 \in \mathbb{R}^2$ at time $t_0 = 0$, that is, $\mathbf{b}(t) = \mathbf{b}_0 + v_\mathrm{b}\mathbf{w}t$, $t \in [0, t_f]$. Let $\mathbf{p}_0 \in \mathbb{R}^2$ be the initial position of the vehicle at time $t_0 = 0$; we assume piecewise constant speed of the vehicle $v_k > v_\mathrm{b}$, $k \in \{0\} \cup \mathbb{I}_{m-2}$.

Fig. 4 shows a numerical solution to this scenario with the beacon moving along the x_1-axis, i.e., $\mathbf{w} = \begin{bmatrix} 1 & 0 \end{bmatrix}^{\mathrm{T}}$, at a constant forward speed of $v_\mathrm{b} = 0.3\,[\mathrm{m/s}]$ starting from $\mathbf{b}_0 = \mathbf{0}$. The sampling time $T = 6\,[\mathrm{s}]$ and the number of samples $m = 6$. The vehicle initial position is $\mathbf{p}_0 = \begin{bmatrix} 0 & -10 \end{bmatrix}^{\mathrm{T}}$ [m]. Fig. 5 shows the time evolution of optimal vehicle speed and course angle for the vehicle.

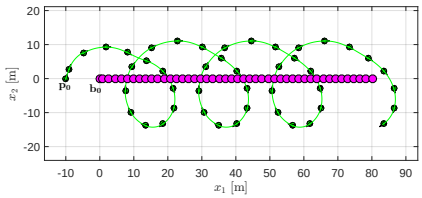

Fig. 4. Optimal trajectory of the vehicle for a beacon moving along a straight-line.

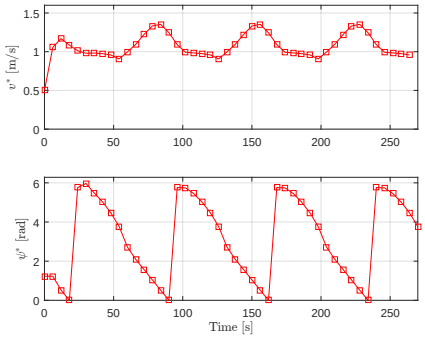

Fig. 5. Evolution of optimal vehicle speed (top) and course angle (below).

5.2 Circular motion

In this case, we consider a beacon moving along a circumference with constant angular speed $\omega_\mathrm{b} > 0$ (clockwise) starting from $v_\mathrm{b}\mathbf{g}(\phi) \in \mathbb{R}^2$, $\phi \in [0, 2\pi)$, $v_\mathrm{b} > 0$, at time $t_0 = 0$. In other words, $\mathbf{b}(t) = v_\mathrm{b}\mathbf{g}(\omega_\mathrm{b}t + \phi)$, $t \in [0, t_f]$.

Fig. 6 shows a numerical solution for the case where $\omega_\mathrm{b} = 0.0131\,[\mathrm{rad/s}]$, $v_\mathrm{b} = 0.3\,[\mathrm{m/s}]$, and $\mathbf{b}_0 = \mathbf{0}$. The sampling time $T = 6\,[\mathrm{s}]$ and the number of samples $m = 6$. The vehicle's initial position is $\mathbf{p}_0 = \begin{bmatrix} -10 & 0 \end{bmatrix}^{\mathrm{T}}$ [m]. Fig. 7 shows the time evolution of optimal vehicle speed and course angle.

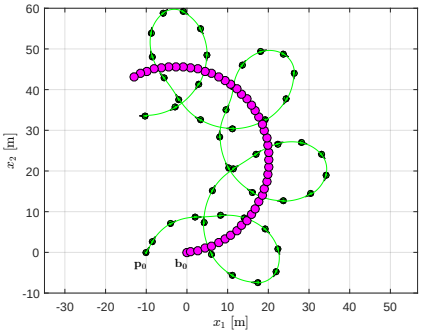

Fig. 6. Optimal trajectory of the vehicle for the beacon moving along an arc of a circumference.

6. TARGET LOCALIZATION: EXPERIMENTAL RESULTS

In Section 5, we considered the problem of computing optimal trajectories of a vehicle for self-positioning using range measurements to a known beacon. We now consider the

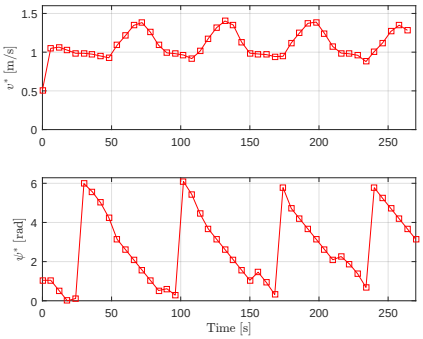

Fig. 7. Evolution of optimal vehicle speed (top) and course angle (below).

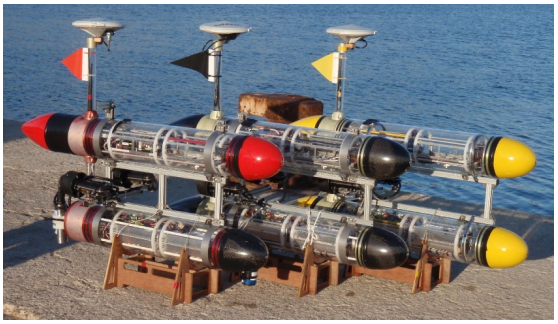

Fig. 8. The MEDUSA-class of marine robotic vehicles.

dual problem of finding optimal trajectories of a vehicle, whose position is known, to localize a target underwater by using range measurements to the target. In the first problem, the vehicle position is unknown and the beacon is known, while in the latter problem the vehicle position is known and that of the target is unknown. However, in both cases the vehicle should optimize its trajectory, either for self-positioning or target localization. From a theoretical standpoint, the computation of optimal vehicle trajectories for target localization is done by adopting a methodology similar to that used in the case of self-positioning. The details are omitted.

In what follows we discuss briefly the implementation of the strategy adopted for target localization and present the results of sea trials using two autonomous marine vehicles of the MEDUSA class (Fig. 8). Each vehicle has two side thrusters that can be independently controlled to impart forward and rotational motion. In addition, they are equipped with an attitude and heading reference system (AHRS) that provides measurement of body orientation and body-fixed angular velocity for control purposes. Each vehicle carries an acoustic Blueprint Seatrac data modem and ranging unit ** that is used for communications and range measurements.Throughout the tests, one of the MEDUSA vehicles was used as an underwater target, while the other was used as a surface vehicle (i.e. tracker, equipped with GPS) interrogating the target. In the missions executed, the target performed a lawnmowing starting from an unknown initial position. The target operated at a constant depth of 1 [m] and a constant body-speed of 0.2 [m/s], and performed dead reckoning navigation using a DVL and the AHRS. In the preliminary experiments performed, the tracker had access to the range to the target and to the velocity vector of the latter (communicated via the acoustic communications channel) every 1.5 [s]. This was done for simplicity of implementation of the algorithm adopted for target localization. In fact, from a theoretical standpoint, one can lift the requirement that the speed of the target be known to the tracker. This issue will be addressed in future experiments.

**http://blueprintsubsea.com/seatrac/index.php

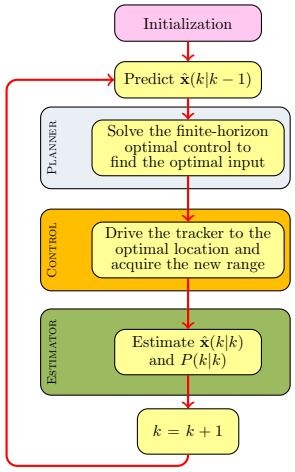

Fig. 9. Integrated motion planning, control, and estimation for range-based target localization: flow chart of the algorithm. Here $\mathbf{x}$ is the state of the target, $\hat{\mathbf{x}}$ its estimate, and P is the estimation error covariance matrix.

Fig. 9 shows the overall block diagram of the algorithm adopted for tracking purposes. The algorithm runs over a sliding time window where tracker motion planning and control, as well as target estimation run sequentially. First, using prior knowledge about the motion of the target, the planner computes optimal values for the piecewise constant tracker speed and course-rate for the next six samples of time, yielding a trajectory (consisting of way point) to be tracked. In the next step the target maneuvers under closed loop control to reach the next way point and acquires a new range measurement. A range-based target localization filter (EKF estimator) is run in parallel onboard the tracker to update the information about the target motion. The process is then repeated.

Fig. 10 shows the plot of the optimal trajectory of the surface vehicle and the estimated trajectory of the target. For comparison purposes, the target trajectory was estimated using two independent sources of information: i) the output of the EKF target localization filter, and ii) the relative position of the target with respect to the tracker as measured by a USBL unit installed on board the latter vehicle. Fig. 11 shows the time-history of the optimal and measured tracker speed. Note that at the beginning of the mission, the measured speed (see Fig. 11) was saturated at the nominal speed 1 [m/s] of the MEDUSA. This was due to fact that motion planning was done by assuming a maximum possible speed of 1.5 [m/s], but the particular tracker used in the field tests could not reach speeds higher than 1.0 [m/s]. Fig. 12 shows the time-history of the course angle, while the Fig. 13 represents the actual measurements. Fig. 14 shows the variance of the position estimates.

Finally, recall from the Proposition 1 that the optimal FIM for the problem at hand is given by $(m\sigma^{-2}/2)I_2$, that is, the off diagonal elements of the FIM are zero, while the diagonal elements are equal and given by $m\sigma^{-2}/2$. Consequently, the optimal determinant of FIM is $m^2\sigma^{-4}/4$. Figs. 15 and 16 show the plot of the evolution of the normalized FIM and normalized determinant versus number of samples, which is consistent with our theoretical findings.

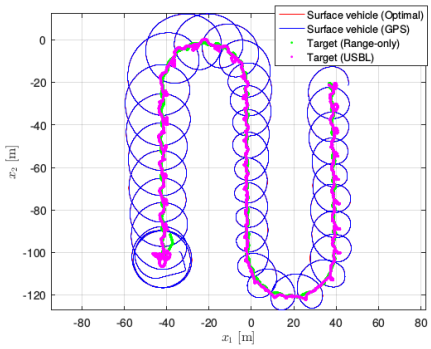

Fig. 10. Optimal tracker and estimated target trajectories.

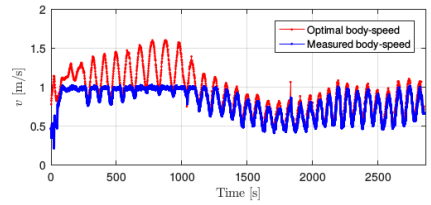

Fig. 11. Tracker speed.

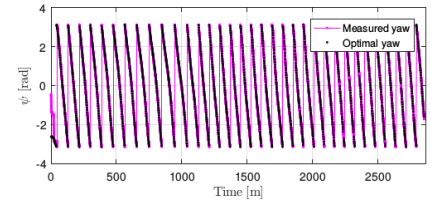

Fig. 12. Optimal course angle for the tracker.

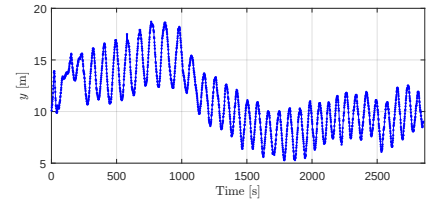

Fig. 13. Range measurements.

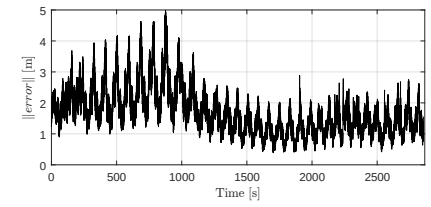

Fig. 14. Variance of tracker position estimates.

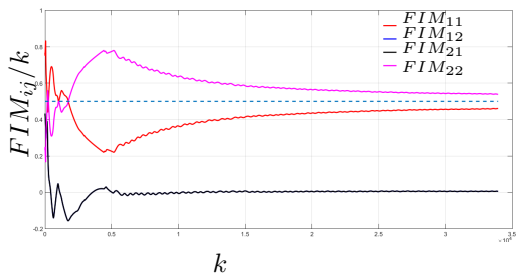

Fig. 15. Components of normalized FIM.

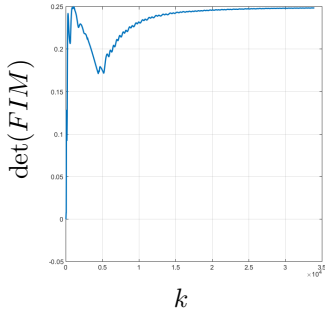

Fig. 16. Determinant of normalized FIM.

7. CONCLUSIONS

The paper derived theoretical results that allow for the computation of optimal marine vehicle trajectories for range-based vehicle positioning and target localization. Building on classical estimation theory, the methodology adopted amounts to maximizing the determinant of an appropriately defined FIM. Experimental results were obtained for the target localization problem, using a surface and an underwater vehicle of the MEDUSA class of marine robots. The results obtained show the efficacy of the method developed for target localization.

ACKNOWLEDGMENTS

The authors are indebted to J. Botelho, P. Góis, J. Ribeiro, M. Rufino, L. Sebastião, and H. Silva for their untiring support and collaboration on the planning and execution of sea trials with the MEDUSA vehicles.

REFERENCES

S. E. Webster, J. M. Walls, L. L. Whitcomb and R. M. Eustice. Decentralized extended information filter for single-beacon cooperative acoustic navigation: Theory and experiments. *IEEE Transactions on Robotics*, 29(4), 957-974, 2013.

N. Crasta, M. Bayat, A. P. Aguiar and A. M. Pascoal. Observability analysis of 3D AUV trimming trajectories in the presence of ocean currents using range and depth measurements. *Annual Reviews in Control*, 40, 142-156, 2015.

M. Bayat, N. Crasta, A. P. Aguiar and A. M. Pascoal. Range-based underwater vehicle localization in the presence of unknown ocean currents: Theory and experiments. *IEEE Transactions on Control Systems Technology*, 24(1), 122-139, 2016.

D. Moreno-Salinas, A. M. Pascoal and J. Aranda. Optimal sensor placement for acoustic underwater target positioning with range-only measurements. *IEEE Journal of Oceanic Engineering*, 41(3), 620-643, 2016.

M. Pedro, D. Moreno-Salinas, N. Crasta, and A. M. Pascoal. Underwater single-beacon localization: Optimal trajectory planning and minimum-energy estimation. *4th IFAC Workshop on Navigation, Guidance and Control of Underwater Vehicles*, Girona, Spain, Apr. 28-30, 2015.

N. D. Powel and K. A. Morgansen. Empirical observability Gramian rank condition for weak observability of nonlinear systems with control. *54th IEEE Conference on Decision and Control*, Osaka, Japan, Dec. 15-18, 2015.

D. Moreno-Salinas, A. M. Pascoal and J. Aranda. Optimal sensor placement for multiple target positioning with range-only measurements in two-dimensional scenarios. *Sensors*, 13, 10674-10710, 2013.

Van Trees and L Harry. *Detection, Estimation and Modulation Theory*. NY: John Wiley and Sons Inc., 1968.